



A Novel Microtubule-Tau Association Enhancer and Neuroprotective Drug Candidate: Ac-SKIP

Yanina Ivashko-Pachima and Illana Gozes*

Dr. Diana and Zelman Elton (Elbaum) Laboratory for Molecular Neuroendocrinology, Department of Human Molecular Genetics and Biochemistry, Sackler Faculty of Medicine, Sagol School of Neuroscience, Adams Super Center for Brain Studies, Tel Aviv University, Tel Aviv, Israel

OPEN ACCESS

Edited by:

Jesus Avila,
Autonomous University of Madrid,
Spain

Reviewed by:

Mar Perez,
Autonomous University of Madrid,
Spain

Francisco G. Wandosell,
Severo Ochoa Molecular Biology
Center (CSIC-UAM), Spain

*Correspondence:

Illana Gozes
igozes@tauex.tau.ac.il;
igozes@post.tau.ac.il

Specialty section:

This article was submitted to
Cellular Neuropathology,
a section of the journal
Frontiers in Cellular Neuroscience

Received: 03 June 2019

Accepted: 12 September 2019

Published: 01 October 2019

Citation:

Ivashko-Pachima Y and Gozes I
(2019) A Novel Microtubule-Tau
Association Enhancer
and Neuroprotective Drug Candidate:
Ac-SKIP.
Front. Cell. Neurosci. 13:435.
doi: 10.3389/fncel.2019.00435

Activity-dependent neuroprotective protein (ADNP) has been initially discovered through its eight amino acid sequence NAPVSIPQ, which shares SIP motif with SALLRSIPA – a peptide derived from activity-dependent neurotrophic factor (ADNF). Mechanistically, both NAPVSIPQ and SALLRSIPA contain a SIP motif that is identified as a variation of SxIP domain, providing direct interaction with microtubule end-binding proteins (EBs). The peptide SKIP was shown before to provide neuroprotection *in vitro* and protect against *Adnp*-related axonal transport deficits *in vivo*. Here we show, for the first time that SKIP enhanced microtubule dynamics, and prevented Tau-microtubule dissociation and microtubule disassembly induced by the Alzheimer's related zinc intoxication. Furthermore, we introduced, CH₃CO-SKIP-NH₂ (Ac-SKIP), providing efficacious neuroprotection. Since microtubule – Tau organization and dynamics is central in axonal microtubule cytoskeleton and transport, tightly related to aging processes and Alzheimer's disease, our current study provides a compelling molecular explanation to the *in vivo* activity of SKIP, placing SKIP motif as a central focus for MT-based neuroprotection in tauopathies with axonal transport implications.

Keywords: tau, microtubules, EBs, ADNP, SKIP

INTRODUCTION

Activity-dependent neuroprotective protein (ADNP) has been initially discovered through its eight amino acid sequence NAPVSIPQ (Bassan et al., 1999), which shares SIP motif with SALLRSIPA – a peptide derived from activity-dependent neurotrophic factor (ADNF) (Brenneman and Gozes, 1996; Zamostiano et al., 1999). ADNF, and then ADNP, have been originally found to mediate neuroprotective and neurotrophic activities of the vasoactive intestinal peptide (VIP) (Brenneman and Gozes, 1996; Brenneman et al., 1998). Subsequent studies have shown that ADNP is dysregulated in schizophrenia (Dresner et al., 2011; Merenlender-Wagner et al., 2015) and Alzheimer's disease (AD) (Yang et al., 2012; Malishkevich et al., 2016), and mutated in autism spectrum disorder (ASD) with 0.17% prevalence (together, these ASD cases are now identified as the ADNP syndrome) (Helsmoortel et al., 2014; Gozes et al., 2015). Importantly, it has been shown that ADNP is the only down-regulated protein in the serum of AD patients (Yang et al., 2012) and expression levels of ADNP in plasma/serum and lymphocyte is correlated with AD clinical progression, disease pathology and premorbid intelligence (Malishkevich et al., 2016). Animal studies with mice expressing *Adnp* from only one allele (*Adnp*[±]) have shown that *Adnp*

deficiency is associated with age-dependent neurodegeneration and cognitive impairment, coupled with tauopathy-like features such as an increase formation of tangle-like structures, defective axonal transport, and Tau hyperphosphorylation (Vulih-Shultzman et al., 2007).

Both peptides NAPVSIQ (ADNP-derived) and SALLRSIPA (ADNF-derived) have shown neuroprotective activities against cognitive decline and peripheral neuropathy in various animal models (Shiryaev et al., 2011; Gozes et al., 2016). NAP biochemical activity has been broadly examined and found to be inextricably linked with microtubules (MTs) and MT-related cellular events: NAP increases MT elongation and dynamics (Ivashko-Pachima et al., 2017), augments axonal transport, in the face of MT deficiencies (Jouroukhin et al., 2013), and protects Tau-MT association under various insults (Oz et al., 2012; Ivashko-Pachima et al., 2017). Mechanistically, both NAPVSIQ and SALLRSIPA contain a SIP motif that is identified as a variation of SxIP domain, providing direct interaction with MT end-binding proteins (EBs) (Honnappa et al., 2009). Our initial studies have shown a direct interaction of SIP- and SKIP-containing peptides with EB1 and EB3 proteins (Oz et al., 2014). We have further shown that four amino acid peptide SKIP docks to the EB3 binding site *in silico*, and stimulates axonal transport *in vivo*, which is reduced as a consequence of *Adnp* deficiency in *Adnp*[±] mice (Amram et al., 2016).

Here, we aimed to test the activity of SKIP and modified SKIP – CH₃CO-SKIP-NH₂ (Ac-SKIP) on MT dynamics and integrity, mediated by MT-associated proteins EB1 and Tau. EB proteins can directly influence MT dynamics (Komarova et al., 2009) and also enroll other MT-affecting proteins to the growing MT plus-ends (Honnappa et al., 2009). Tau is a broadly known MT-associated protein which stimulates MT assembly and Tau physiological and biochemical impairments are well-studied in a variety of neurodegenerative diseases, referred to tauopathies (Kneynsberg et al., 2017). Furthermore, it has been found that Tau directly associates with EB1 and EB3 proteins and modulates their location on the MTs (Sayas et al., 2015). Here, we tested different concentrations of SKIP and Ac-SKIP and found that at 10⁻⁹ M SKIP and Ac-SKIP exhibited consistent and significant activity: (1) increased elongation of freshly growing MT plus-ends; and prevented, (2) Tau-MT dissociation, and (3) MT disassembly, induced by extracellular zinc. Thus, our current study provided a molecular explanation to the previously observed effect of SKIP on MT-related functions: stimulation of axonal transport and normalization of social memory in *Adnp* ± mice. Furthermore, our results showed that Ac-SKIP provided surprisingly more efficacious neuroprotection and suggested that SKIP might be the shortest motif essential for MT-based neuroprotection, mediated by EB proteins and Tau.

MATERIALS AND METHODS

Cell Culture and Treatments

Mouse neuroblastoma N1E-115 cells (ATCC, Bethesda, MD, United States) were maintained in Dulbecco's modified Eagle's medium (DMEM), 10% fetal bovine serum (FBS),

2 mM glutamine and 100 U/ml penicillin, 100 mg/ml streptomycin (Biological Industries, Beit Haemek, Israel). Human neuroblastoma SH-SY5 cells (ECACC, Public Health England, Porton Down, Salisbury, United Kingdom; passage numbers from 14 to 16) were maintained in Ham's F12: minimum essential media (MEM) Eagle (1:1), 2 mM Glutamine, 1% non-essential amino acids, 15% FBS and 100 U/ml penicillin, 100 mg/ml streptomycin (Biological Industries, Beit Haemek, Israel). Cells were incubated in 95% air/5% CO₂ in a humidified incubator at 37°C. Cells were differentiated with reduced FBS (2%) and DMSO (1.25%) containing medium (N1E-115 cells) or with retinoic acid at a concentration of 10 μM (SH-SY5Y cells) during 7 days before each experiment. Differentiated N1E-115 cells were treated for 2 or 4 h with SKIP/Ac-SKIP in final concentrations of 10⁻¹² – 10⁻⁶ M, in the absence or presence of zinc (400 μM of ZnCl₂, stock solution – 0.1 M ZnCl₂ in water, Sigma, Rehovot, Israel).

Cell Viability Assay

A week before the experiment, N1E-115 cells were plated onto 96-well plates at a concentration of 5000 cells/well in 100 μl of the growth medium, which was replaced by differentiation medium a day after cell seeding. On an experimental day, cells were treated during 4 h with 400 μM of ZnCl₂ in the absence or presence of NAP (10⁻¹² – 10⁻⁹ M). Cell survival was measured using XTT-based cell proliferation kit (Biological Industries, Beit Haemek, Israel), which was performed according to the manufacturer's instructions. The absorbance of the samples was measured with a spectrophotometer (ELISA reader) at wavelengths of 490/630 nm.

Time-Lapse Imaging of EB1 Comet-Like Structures

N1E-115 cells were plated on 35 mm dishes (81156, μ-Dish, Ibidi, Martinsried, Germany) at a concentration of 25000 cells/dish and then differentiated with reduced FBS, DMSO-containing medium during seven days. 48 h before live imaging, differentiated N1E-115 cells were transfected with 1 μg of EB1-RFP expressing plasmid. On an experimental day, N1E-115 cells were incubated at 37°C with a 5% CO₂/95% air mixture in a thermostatic chamber placed on the stage of a Leica TCS SP5 confocal microscope (objective ×100 (PL Apo) oil immersion, NA 1.4). Time-lapse images were automatically captured every 3 s during 2 min, using the Leica LAS AF software (Leica Microsystems, Wetzlar, Germany). Data were collected and analyzed by Imaris software (Bitplane, Concord, MA, United States).

Fluorescence Recovery After Photobleaching

Forty-eight hours before a fluorescence recovery after photobleaching (FRAP) experiment, differentiated N1E-115 cells were transfected with a 1 μg pmCherry-C1-Tau3R plasmid (Ivashko-Pachima et al., 2019). FRAP was performed using a Leica TCS SP5 confocal microscope [objective 100× (PL Apo) oil immersion, NA 1.4]. ROIs (regions of interest) for

photobleaching were drawn in the proximal cell branches. mCherry-Tau molecules were bleached with argon laser during 15 s, and data about fluorescence recovery after bleaching were automatically collected (80 images every 0.74 s) by the Leica LAS AF software. Fluorescence intensities were measured by ImageJ Fiji (Schindelin et al., 2012), obtained data were normalized with easyFRAP software (Rapsomaniki et al., 2012). FRAP recovery results were fitted by a one-phase exponential association function and recovery curves were built using GraphPad Prism 6 (GraphPad Software, Inc., La Jolla, CA). Samples with $R^2 < 0.9$ were excluded.

Polymerized vs. Soluble Tubulin Quantification Assay

Quantification of tubulin polymerization was performed as previously (Oz et al., 2012; Ivashko-Pachima et al., 2017; Ivashko-Pachima and Gozes, 2018). Briefly, in order to extract soluble tubulin (S) differentiated N1E-115 cells were lysed with TritonX-100-containing MT-buffer (80 mM PIPES pH6.8, 1 mM $MgCl_2$, 2 mM EGTA, 5% Glycerol, with or without 0.5% TritonX-100) at room temperature for 5 min while centrifuging at 800 rcf; in order to collect the polymerized tubulin (P) pelleted cells were rinsed once again with equal volume of modified RIPA buffer (50 mM Tris-HCl pH7.4, 150 mM NaCl, 2 mM EGTA, 1% TritonX-100, 0.1% SDS, 0.1% sodium Deoxycholate, protease and phosphatase inhibitors: 1 mM phenylmethylsulphonyl-fluoride (PMSF), leupeptin 25 μ g/ml, pepstatin 25 μ g/ml, Na_3VO_4 1 mM, NaF 20 mM) on ice. The soluble and polymerized tubulin fractions were each mixed with the same amount of sample buffer (10 mM Tris-HCl, pH6.8, 1.5% SDS, 0.6% DTT and 6% (v/v) glycerol) and heated at 95°C for 5 min. An equal volume of each fraction was analyzed by immunoblotting with appropriate antibodies, and the results following ECL development (by a chemiluminescence kit, Pierce, Rockford, IL, United States) were quantified by densitometry (using GelQuant.NET software provided by biochemlabsolutions.com).

Co-immunoprecipitation Assay

Proteins were extracted from differentiated human neuroblastoma SH-SY5Y cells and Co-IP assay was performed as previously reported (Merenlender-Wagner et al., 2015; Ivashko-Pachima et al., 2017) using Co-IP kit according to the manufacture protocol (Pierce, Rockford, IL, United States). Briefly, 10 μ g of antibodies of interest (EB1, ab53358, Abcam, Cambridge, United Kingdom; and total Tau antibody, AT-5004, MBL, Billerica, MA, United States) were cross-linked to the 30 μ l of A/G PLUS-agarose beads (provided by the Co-IP kit). 2 μ g of SKIP or Ac-SKIP, diluted into lysis buffer were added per sample (1 mg of cell lysate) for 2 h at room temperature. Flow-through, wash and elution fractions were then collected and analyzed by immunoblotting with appropriate antibodies, and the results following ECL (Pierce) development were quantified by densitometry (GelQuant.NET software provided by biochemlabsolutions.com).

Antibody List

Tubulin – monoclonal α -tubulin antibody (mouse IgG1 isotype, T6199, Sigma, Rehovot, Israel). Actin – mouse monoclonal actin antibody (Sigma, Rehovot, Israel). The secondary antibodies were peroxidase-conjugated AffiniPure goat anti-mouse IgG (Jackson ImmunoResearch, United States).

Statistical Analysis

Data are presented as the mean \pm SEM from at least 3 independent experiments performed in triplicates. Statistical analysis of the data was performed by using one-way ANOVA test (followed by the Turkey or LSD *post hoc* test) by IBM SPSS Statistics software version 23 (IBM, Armonk, NY, United States). * $P < 0.05$, ** $P < 0.01$, *** $P < 0.001$. Detailed statistical data are summarized in the **Supplementary File**.

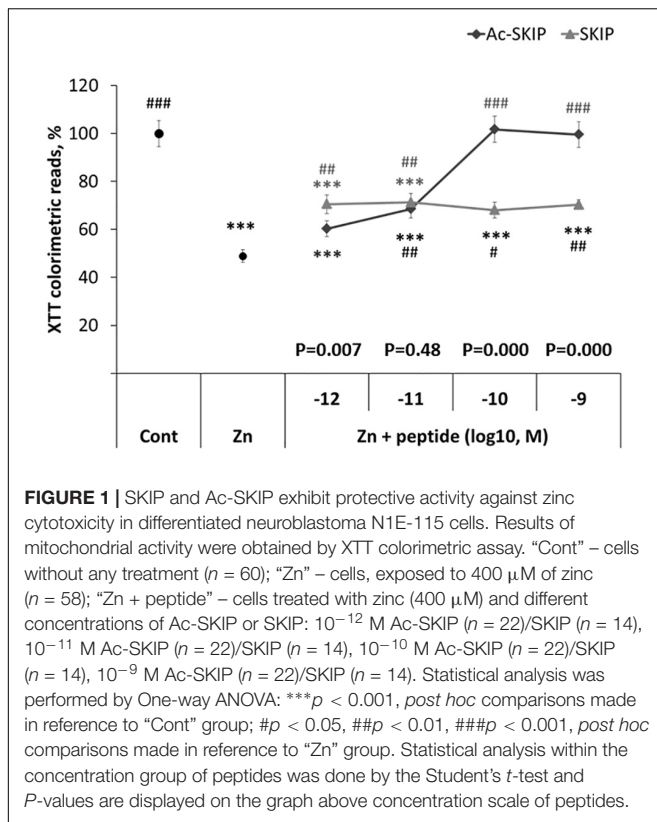
RESULTS

The Protective Effect of SKIP and Ac-SKIP Against Cell Death Induced by Zinc Toxicity

A colorimetric method for cell viability (based on the tetrazolium salt – XTT) was used to assess the protective activity of SKIP and Ac-SKIP at different concentrations (10^{-12} – 10^{-9} M) against the cytotoxic effect of zinc in order to choose potent concentration for the further experiments. Differentiated neuroblastoma N1E-115 cells were treated with zinc alone or together with Ac-SKIP or SKIP for 4 h, and XTT-produced soluble dye was then measured by ELISA reader. Previously published data have shown a consistent and significant effect of zinc cytotoxicity at 400 μ M (Sanchez-Martin et al., 2010; Oz et al., 2012; Ivashko-Pachima et al., 2017). Hence, here, we worked with 400 μ M of zinc. Treatment with zinc caused a reduction of ~50% in cell viability, and peptide treatments showed significant protection against cell death, except for Ac-SKIP at 10^{-12} M. SKIP treatment at every examined concentration exhibited nearly equal ~20% protection that was found statistically significant. Ac-SKIP protective potency was found to be positively dependent on the peptide concentration: non-significant slight protection at 10^{-12} M; significant, a moderate effect at 10^{-11} M; and a ~100% protective effect at 10^{-10} M and 10^{-9} M. Ac-SKIP and SKIP exhibited the same protective potency at 10^{-11} M and significantly different magnitude of protective activity at 10^{-12} M (with a greater effect of SKIP), 10^{-10} M and 10^{-9} M (with a significantly greater effect of Ac-SKIP). For further experiments, we chose to work with 10^{-12} M and 10^{-9} M of Ac-SKIP/SKIP (**Figure 1**).

Ac-SKIP and SKIP Affect MT Dynamics

The direct interaction between SKIP and EB1/3 has been previously predicted by Pymol (Schrödinger, 2015), and peptides containing SxIP motif have displayed the association with EB1/3 in sulfolink columns. Here, we aimed to evaluate the effect of SKIP and Ac-SKIP on MT dynamics, mediated by direct interaction of these peptides with the EB1 protein. Differentiated



neuroblastoma cells were subjected to transient transfection with expression plasmid encoding to EB1 protein, tagged to RFP (Figure 2A and Supplementary Figure S1). Single-cell time-lapse imaging allowed the evaluation of the effect of the peptides on MT dynamics by tracking RFP-EB1 comet-like structures decorating newly polymerized MT plus-ends. Time-lapse imaging followed by the 4 h peptide treatment with Ac-SKIP or SKIP showed that both Ac-SKIP and SKIP at 10^{-9} M (but not at 10^{-12} M) significantly augmented the track length (Figure 2B) and velocity (Figure 2C) of the EB1 comets, reflecting the lengths of the MT growing events and the speed of MT assembly, respectively. Thus, both peptides had an impact on MT dynamics.

Protective Effect of Ac-SKIP and SKIP on Tau-MT Association, Disrupted by Zinc

In order to evaluate the protective activity of Ac-SKIP and SKIP against Tau-MT discharge we performed FRAP assay using zinc as Tau-MT dissociation agent (Craddock et al., 2012; Huang et al., 2014). Differentiated N1E-115 cells were transfected with a plasmid expressing mCherry-tagged Tau protein, and FRAP imaging (Figure 3A and Supplementary Figure S2) was performed after an hour of cell exposure to zinc alone or together with Ac-SKIP or SKIP (10^{-12} M, 10^{-9} M). MT regions decorated by mCherry-Tau were bleached (Figure 3A, marked squares, 0 s after bleaching) and recovery of mCherry fluorescence (Figure 3A, marked squares, 88 s after bleaching) resulted from interchange between MT-bound Tau (carrying bleached mCherry molecules) and previously unbound Tau

proteins (carrying unbleached mCherry molecules). Thus, an unrecovered fraction of the initial mCherry fluorescence within a given bleached area indicated the immobile fraction mCherry-Tau proteins, reflecting Tau interaction with MTs. Subsequent analysis of the data obtained with a one-phase exponential association (Figures 3B,C) showed that zinc significantly abated Tau immobile fraction in comparison to the non-treated control (Figures 3B,C). Ac-SKIP and SKIP at both examined concentrations (10^{-12} M and 10^{-9} M) prevented excessive Tau release from MTs, induced by zinc, which was found statistically significant in comparison to zinc treatment alone (Figures 3B,C).

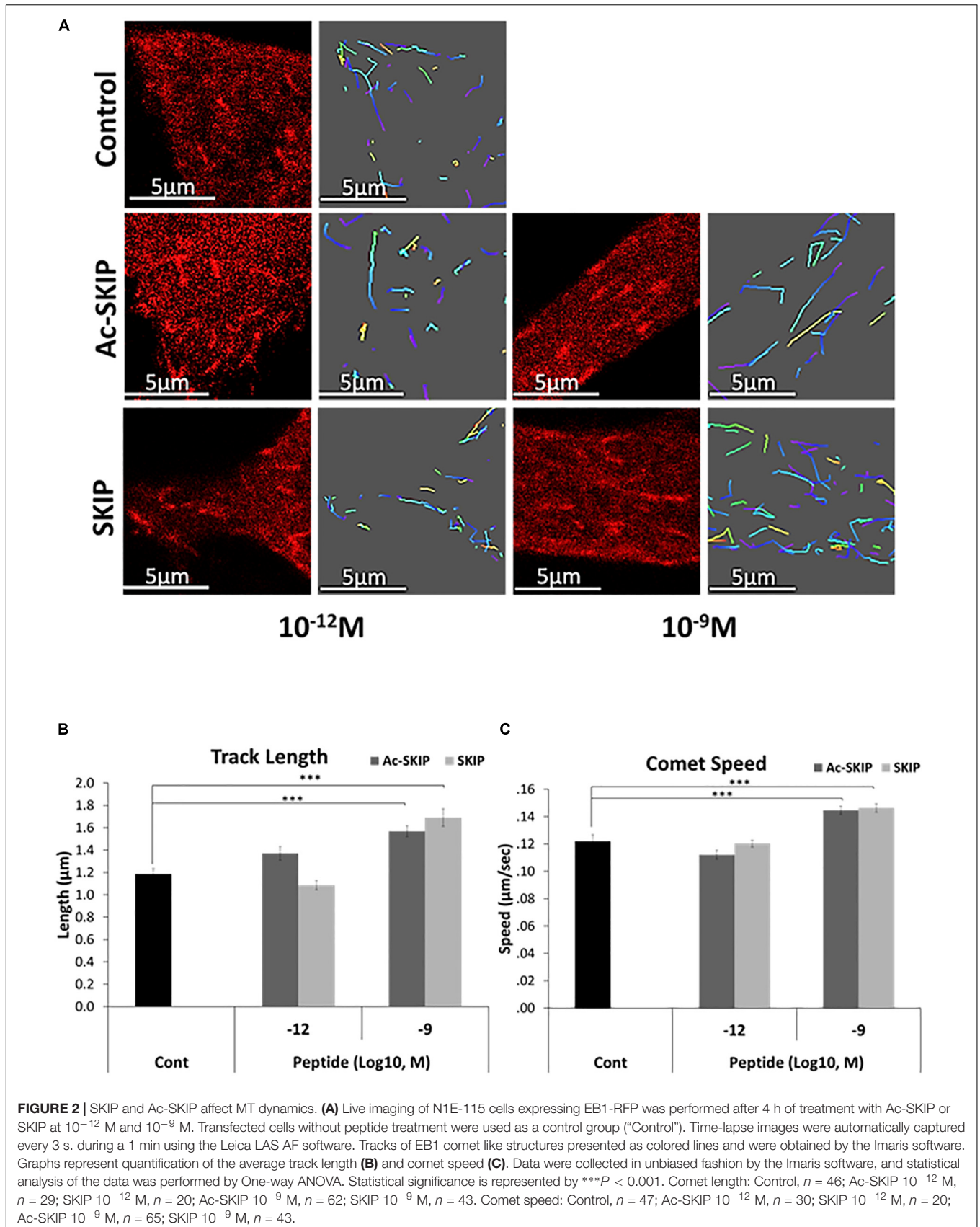
Ac-SKIP and SKIP Prevent MT Disassembly, Induced by Zinc Intoxication

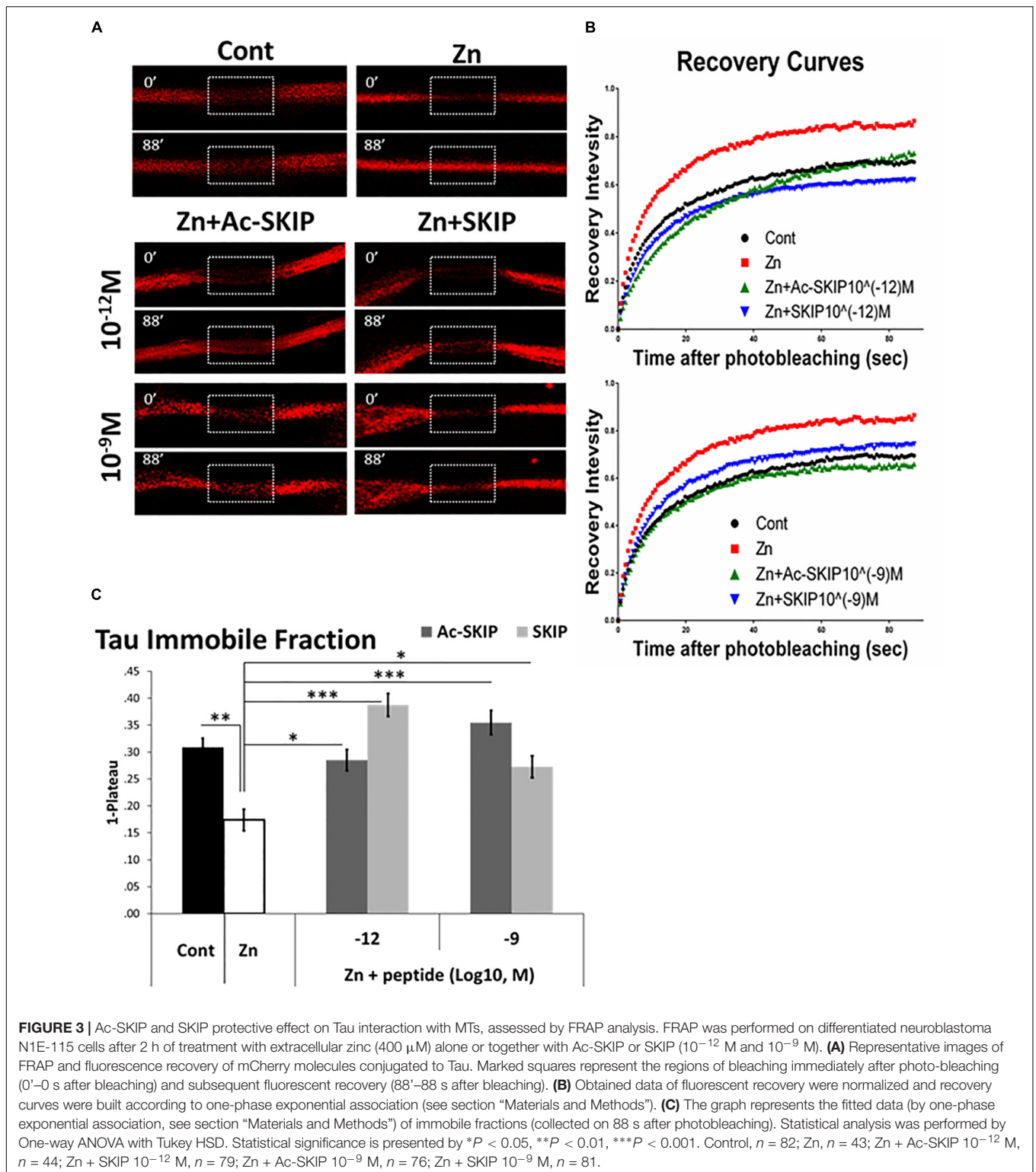
Further, we aimed to determine the protective effect of Ac-SKIP and SKIP against MT disassembly induced by zinc as an MT disruptor. We examined the relative levels of polymerized and soluble tubulin pools in differentiated N1E-115 cells, exposed to extracellular zinc (400 μM) alone or together with Ac-SKIP or SKIP (10^{-12} M and 10^{-9} M). After treatment cells were lysed (as described in section “Materials and Methods” section) and the tubulin levels of polymerized and soluble fractions were evaluated by western blotting (Figure 4A, Tubulin panel, and Supplementary Figure S3A) followed by densitometric quantification (Figure 4B). Non-treated control cells exhibited a nearly equal distribution of tubulin between soluble (S) and polymerized (P) fractions, while zinc treatment significantly increased the ratio of soluble to polymerized tubulin content (Figure 4A, Tubulin panel; Figure 4B). Ac-SKIP or SKIP added together with zinc exhibited reduced the tubulin content in the soluble fraction compared to “zinc” group, which was found statistically significant for all peptide treatments, except for Ac-SKIP at 10^{-12} M (Figure 4A, Tubulin panel; Figure 4B).

There was no observed effect on the actin-microfilament pool following neither zinc nor Ac-SKIP/SKIP treatment (Figure 4A, Actin panel, and Supplementary Figures S3B, S4), suggesting that zinc/Ac-SKIP/SKIP had selective effects on the MT cytoskeleton.

SKIP/Ac-SKIP Enhance Tau-EB1 and Tau-Tubulin Interactions

To study the effect of SKIP and Ac-SKIP on the crosstalk between EB1-Tau and -tubulin, we performed co-immunoprecipitation (Co-IP) assays in differentiated human neuroblastoma SH-SY5Y cells as previously reported (Merenlender-Wagner et al., 2015; Ivashko-Pachima et al., 2017). We examined the effect of SKIP and Ac-SKIP on EB1-Tau interaction by protein complex immunoprecipitation (Co-IP) assays, using EB1 and Tau antibodies linked to agarose beads (Figure 4C, IP: EB1; Figure 4D, IP: Tau). The elution fractions, obtained from immunoprecipitations (IPs) performed with either anti-EB1 or anti-Tau, were analyzed by immunoblotting (IB) with EB1 and Tau antibodies (Figure 4C, IP: EB1 IB: Tau; Figure 4D, IP: Tau IB: EB1). Results showed that both SKIP and Ac-SKIP increased Tau-EB1 association, compared to the samples





incubated without these peptides (**Figure 4C**, IP: EB1 Cont – control, IB: Tau; **Figure 4D**, IP: Tau Cont IB: EB1). IP: EB1 IB: EB1 showed a significant increase in EB1-EB1 interaction (EB1 homodimer formation) following SKIP treatment and moderate non-significant increase following Ac-SKIP, compared to the

control (**Figure 4C**, IP: EB1 Cont IB: EB1). IP: Tau IB: Tau did not show significant differences in Tau-Tau association following incubation with either SKIP or Ac-SKIP (**Figure 4D**). Further immunoblotting analysis with tubulin antibodies suggested increased Tau-tubulin, interaction following treatments with

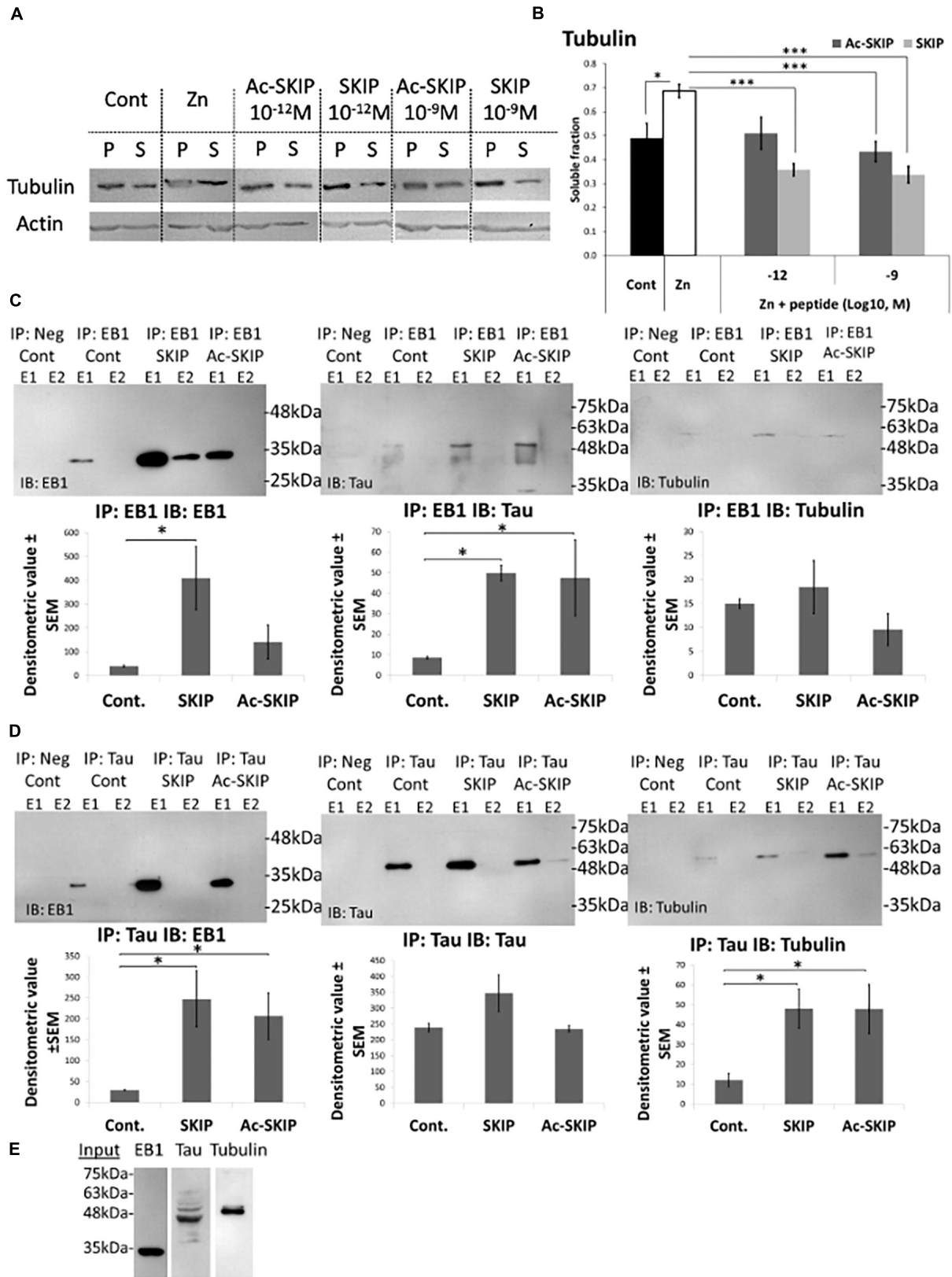


FIGURE 4 | Continued

FIGURE 4 | Ac-SKIP and SKIP effect on the polymerized vs. the soluble tubulin pool and the crosstalk between EB-Tau-tubulin. **(A)** Immunoblotting of polymerized (P) and soluble (S) protein fractions (obtained by polymerized vs. soluble tubulin assay, see section “Materials and Methods”) with tubulin antibodies. Cells were treated with zinc (400 μ M, 4 h) with or without Ac-SKIP or SKIP (10^{-12} M and 10^{-9} M, 4 h), non-treated cells served as controls. **(B)** The graph represents the densitometric quantification of soluble tubulin ratios. The intensity of each band was quantified by densitometry and the soluble protein ratio was calculated by dividing the densitometric value of soluble proteins by the total protein content (S/(S + P)). Statistical analysis was performed by One Way ANOVA with Tukey HSD. * $P < 0.05$, ** $P < 0.01$, *** $P < 0.001$; Control, $n = 15$; Zn, $n = 18$; Zn + Ac-SKIP 10^{-12} M, $n = 15$; Zn + SKIP 10^{-12} M, $n = 9$; Zn + Ac-SKIP 10^{-9} M, $n = 18$; Zn + SKIP 10^{-9} M, $n = 11$. **(C,D)** A Co-IP assay was performed with EB1 or Tau antibodies, linked to agarose beads. SKIP (2 μ g/sample) or Ac-SKIP (2 μ g/sample), diluted into Pierce lysis buffer (see section “Materials and Methods”) or the equal volume of lysis buffer w/o peptides (IP: EB1 Cont; IP: Tau Cont) were added to cell lysate of differentiated SH-SY5Y cells, 15 min before EB1 or Tau column application (IP: EB1; IP: Tau). Sequential IP elution fractions (E1, E2) were further analyzed by immunoblotting with EB1, Tau, and Tubulin antibodies (IB: EB1; IB: Tau; IB: Tubulin). In addition, columns with free agarose beads were used as negative controls (IP: Neg cont). The intensity of each band was quantified by densitometry. The bar graph shows the ratio of band intensities (densitometric value \pm SEM) obtained upon SKIP and Ac-SKIP treatments as compared with non-treated cells (Cont). Statistical analysis was performed by One Way ANOVA with LSD HSD. Experiments were independently repeated three times. * $P < 0.05$, ** $P < 0.01$, *** $P < 0.001$. **(E)** Cell lysates without column exposure were used as positive controls (Input). IP – immunoprecipitation, IB – immunoblot.

SKIP and Ac-SKIP (**Figure 4D**, IP: Tau IB: tubulin), while EB1-tubulin association remained without significant changes (**Figure 4C**, IP: EB1 IB: tubulin). Cell lysates without column exposure were used as positive controls (Input, **Figure 4E**) and flow-through and washing fractions were also collected and analyzed by immunoblotting with EB1 and Tau antibodies (**Supplementary Figure S5A**, IP: EB1 IB: EB1; **Supplementary Figure S5B**, IP: Tau IB: Tau).

DISCUSSION

Maintenance of axonal structure and transport underlies neuronal signal transduction and connectivity, and provide a proper brain function (Rasband, 2010). It has been well-established that axonal degeneration (axonopathy) is a central pathogenic feature common to numerous human tauopathies, including AD (Kneynsberg et al., 2017). Atrophy of axon-reach white matter is significant in patients with mild cognitive impairment and extends widely in advanced AD cases, while the degree of atrophy is associated with loss of cognitive functioning (Huang and Auchus, 2007). Furthermore, immunohistochemical analyses of AD brains have revealed that formation of neuropil threads (Tau inclusions within dystrophic neurites) are a prominent AD neuropathological feature that appears before neurofibrillary tangles (NFTs) (Kowall and Kosik, 1987). Mechanistically, a clear correlation between Tau lesions and axonopathy has been demonstrated by multiple models, linking aberrant phosphoregulation of Tau to alterations in axonal transport, and deficits in axonal transport to dying-back degeneration of neurons (Kanaan et al., 2011, 2012, 2013).

The functional repertoire of Tau includes, among other characteristics, regulation of EB protein localization on MTs (Sayas et al., 2015). EBs are MT plus-end tracking proteins that decorate growing MT ends and recruit a variety of other proteins that connect MTs to various cellular structures (Jiang et al., 2012) and control MT dynamics (Komarova et al., 2009). EB-binding proteins directly interact with EBs through a core SxIP motif (Honnappa et al., 2009).

We have previously shown that EB1/3-targeting SKIP ameliorates impaired axonal transport and social memory deficits in the face of *Adnp* deficiency (*Adnp*[±] mice) (Amram et al., 2016). Our current study focused on the molecular activity of

SKIP and Ac-SKIP on the cellular compartment, relevant to the axonal transport – MTs, and MT-associated proteins Tau and EB1. We showed that SKIP and Ac-SKIP significantly increased the elongation and growth rate of MT plus-ends, mediated by EB1 proteins. Furthermore, the protective activity of SKIP and Ac-SKIP on Tau-MT interaction and MT integrity was assessed in the face of zinc intoxication. The well-established hypothesis of zinc dyshomeostasis in AD suggests aberrant zinc accumulation by A β -amyloid plaques, resulting in too low, or excessively high intracellular zinc concentrations (up to 1 mM) in zinc-enriched brain regions implicated in the cognitive functions and vulnerable to AD pathology (Deibel et al., 1996; Craddock et al., 2012; DeGrado et al., 2016). It has been suggested that high intracellular zinc concentrations (more than 100 μ M) present adverse effects on nerve fibers during stimulation (Minami et al., 2006) and may lead to pathological implications and neuronal cell death (Frederickson et al., 2005; Sensi et al., 2009, 2011; Shuttleworth and Weiss, 2011). In addition, it has been shown that abnormally high concentrations (up to 250 μ M) of zinc induce GSK-3 β activation and Tau release from MTs (Boom et al., 2009). Neuronal loss has been observed when zinc levels reached 10–100 nM in the neuronal soma *in vitro* (Aizenman et al., 2000; Jiang et al., 2001; Bossy-Wetzel et al., 2004) and zinc influx of 300 μ M causes ischemic neurodegeneration in rat brains and cortical cultures (Koh et al., 1996). It has also been found that NFTs and amyloid-beta (A β) plaques contain abnormally high levels of zinc (Bush et al., 1994a; Lee et al., 2018). Furthermore, it has been demonstrated that A β 1–40 (a major component of AD cerebral amyloid) specifically and in a saturable fashion binds zinc (Bush et al., 1994b) that could accelerate the A β plaques formation at 200 μ M of zinc (Lee et al., 2018).

Here, we demonstrated an effect of SKIP and Ac-SKIP on the crosstalk between Tau, EB1, and MTs. In this respect, it has been previously shown that Tau directly interacts with EB proteins, modulating MT dynamics (Sayas et al., 2015). Based on the observed results, we suggest that the effect of SKIP and Ac-SKIP on MTs integrity and dynamics is mediated by increasing interaction between EB1 and Tau that is accompanied by the increased association of Tau with tubulin. In addition, SKIP and Ac-SKIP (the last with more moderate effect) enhance EB1 homodimer formation. EB proteins form homo- and heterodimers and play a master role in organizing dynamic protein networks in mammalian cells

(Akhmanova and Steinmetz, 2015). EB1 homodimers have a higher affinity to the p150^{glued} – N-terminal CAP-Gly domain of the dynactin (Honnappa et al., 2006; Bjelic et al., 2012), which in turn acts as a co-factor for the MT motor protein dynein. EB1-dependent ordered recruitment of dynactin to the MT plus-end is required for efficient initiation of retrograde axonal transport (Moughamian et al., 2013). Furthermore, actin-MT linkers – spectraplakins promote axonal growth in an EB1-dependent manner and stabilize MTs in the face of pharmacologically induced depolymerization (Alves-Silva et al., 2012). Thus, increased EB1 homodimer formation by SKIP/Ac-SKIP may have a direct effect on axonal retrograde transport, axonal growth, and neuroprotection.

The differential potency and efficacy of SKIP and Ac-SKIP might be attributed to potential steric hindrance of the modified SKIP at low concentration, and differential residence time at higher concentrations affecting cellular survival. Regardless, since MT organization and dynamics is central in axonal MT cytoskeleton and transport our current study provided a compelling molecular explanation to the *in vivo* activity of SKIP, placing SKIP motif as a central focus for MT-based neuroprotection in tauopathies with axonal transport implication. As MT reduction in AD and aging is independent of Tau filament formation (Cash et al., 2003), our studies implicate a paucity/dysregulation of EB-interacting endogenous proteins, like ADNP (Oz et al., 2014; Malishkevich et al., 2016) as a contributing mechanism and further provides hope with SKIP-containing drug candidates in future *in vivo* studies.

DATA AVAILABILITY STATEMENT

All datasets generated for this study are included in the manuscript/**Supplementary Files**.

REFERENCES

- Aizenman, E., Stout, A. K., Hartnett, K. A., Dineley, K. E., McLaughlin, B., and Reynolds, I. J. (2000). Induction of neuronal apoptosis by thiol oxidation: putative role of intracellular zinc release. *J. Neurochem.* 75, 1878–1888. doi: 10.1046/j.1471-4159.2000.0751878.x
- Akhmanova, A., and Steinmetz, M. O. (2015). Control of microtubule organization and dynamics: two ends in the limelight. *Nat. Rev. Mol. Cell Biol.* 16, 711–726. doi: 10.1038/nrm4084
- Alves-Silva, J., Sanchez-Soriano, N., Beaven, R., Klein, M., Parkin, J., Millard, T. H., et al. (2012). Spectraplakins promote microtubule-mediated axonal growth by functioning as structural microtubule-associated proteins and EB1-dependent +TIPs (tip interacting proteins). *J. Neurosci.* 32, 9143–9158. doi: 10.1523/JNEUROSCI.0416-12.2012
- Amram, N., Hacoheh-Kleiman, G., Sragovich, S., Malishkevich, A., Katz, J., Touloumi, O., et al. (2016). Sexual divergence in microtubule function: the novel intranasal microtubule targeting SKIP normalizes axonal transport and enhances memory. *Mol. Psychiatry* 21, 1467–1476. doi: 10.1038/mp.2015.208
- Bassan, M., Zamostiano, R., Davidson, A., Pinhasov, A., Giladi, E., Perl, O., et al. (1999). Complete sequence of a novel protein containing a femtomolar-activity-dependent neuroprotective peptide. *J. Neurochem.* 72, 1283–1293. doi: 10.1046/j.1471-4159.1999.0721283.x
- Bjelic, S., De Groot, C. O., Scharer, M. A., Jaussi, R., Bargsten, K., Salzmann, M., et al. (2012). Interaction of mammalian end binding proteins with CAP-Gly domains of CLIP-170 and p150^{glued}. *J. Struct. Biol.* 177, 160–167. doi: 10.1016/j.jsb.2011.11.010

AUTHOR CONTRIBUTIONS

YI-P designed and performed the work and wrote the initial draft. IG inspired the project, guided the progress, provided all the required support, and finalized the manuscript.

FUNDING

IG work was supported in part by the following grants, ISF 1424/14, ERA-NET neuron AUTISYN and ADNPinMED, BSF-NSF 2016746, AMN Foundation as well as Drs. Ronith and Armand Stemmer, Mr. Arthur Gerbi (French Friends of Tel Aviv University), Ms. Alicia Koplowitz Foundation (Spanish Friends of Tel Aviv University).

ACKNOWLEDGMENTS

IG is the incumbent of the Lily and Avraham Gildor Chair for the Investigation of Growth Factors, and the Director of the Dr. Diana and Zelman Elton (Elbaum) Laboratory for Molecular Neuroendocrinology at Tel Aviv University. We thank Dr. Laura Sayas for her excellent collaboration and teaching us the microtubule dynamics methodology. This work is in partial fulfillment of the Ph.D. thesis requirements of Ms. Yanina Ivashko-Pachima and Ms. Alicia Koplowitz fellowship.

SUPPLEMENTARY MATERIAL

The Supplementary Material for this article can be found online at: <https://www.frontiersin.org/articles/10.3389/fncel.2019.00435/full#supplementary-material>

- Boom, A., Authelet, M., Dedecker, R., Frederick, C., Van Heurck, R., Daubie, V., et al. (2009). Bimodal modulation of tau protein phosphorylation and conformation by extracellular Zn²⁺ in human-tau transfected cells. *Biochim. Biophys. Acta* 1793, 1058–1067. doi: 10.1016/j.bbamcr.2008.11.011
- Bossy-Wetzel, E., Talantova, M. V., Lee, W. D., Scholzke, M. N., Harrop, A., Mathews, E., et al. (2004). Crosstalk between nitric oxide and zinc pathways to neuronal cell death involving mitochondrial dysfunction and p38-activated K⁺ channels. *Neuron* 41, 351–365. doi: 10.1016/s0896-6273(04)00015-17
- Brenneman, D. E., Glazner, G., Hill, J. M., Hauser, J., Davidson, A., and Gozes, I. (1998). VIP neurotrophism in the central nervous system: multiple effectors and identification of a femtomolar-acting neuroprotective peptide. *Ann. N. Y. Acad. Sci.* 865, 207–212. doi: 10.1111/j.1749-6632.1998.tb11180.x
- Brenneman, D. E., and Gozes, I. (1996). A femtomolar-acting neuroprotective peptide. *J. Clin. Invest.* 97, 2299–2307. doi: 10.1172/JCI118672
- Bush, A. I., Pettingell, W. H. Jr., de Paradis, M., Tanzi, R. E., and Wasco, W. (1994a). The amyloid beta-protein precursor and its mammalian homologues. Evidence for a zinc-modulated heparin-binding superfamily. *J. Biol. Chem.* 269, 26618–26621.
- Bush, A. I., Pettingell, W. H., Multhaup, G., d Paradis, M., Vonsattel, J. P., Gusella, J. F., et al. (1994b). Rapid induction of Alzheimer A beta amyloid formation by zinc. *Science* 265, 1464–1467. doi: 10.1126/science.8073293
- Cash, A. D., Aliev, G., Siedlak, S. L., Nunomura, A., Fujioka, H., Zhu, X., et al. (2003). Microtubule reduction in Alzheimer's disease and aging is independent of tau filament formation. *Am. J. Pathol.* 162, 1623–1627.

- Craddock, T. J., Tuszyński, J. A., Chopra, D., Casey, N., Goldstein, L. E., Hameroff, S. R., et al. (2012). The zinc dyshomeostasis hypothesis of Alzheimer's disease. *PLoS One* 7:e33552. doi: 10.1371/journal.pone.0033552
- DeGrado, T. R., Kemp, B. J., Pandey, M. K., Jiang, H., Gunderson, T. M., Linscheid, L. R., et al. (2016). First PET imaging studies with ⁶³Zn-zinc citrate in healthy human participants and patients with Alzheimer disease. *Mol. Imaging* 15:1536012116673793. doi: 10.1177/1536012116673793
- Deibel, M. A., Ehmann, W. D., and Markesbery, W. R. (1996). Copper, iron, and zinc imbalances in severely degenerated brain regions in Alzheimer's disease: possible relation to oxidative stress. *J. Neurol. Sci.* 143, 137–142. doi: 10.1016/s0022-510x(96)00203-1
- Dresner, E., Agam, G., and Gozes, I. (2011). Activity-dependent neuroprotective protein (ADNP) expression level is correlated with the expression of the sister protein ADNP2: deregulation in schizophrenia. *Eur. Neuropsychopharmacol.* 21, 355–361. doi: 10.1016/j.euroneuro.2010.06.004
- Frederickson, C. J., Koh, J. Y., and Bush, A. I. (2005). The neurobiology of zinc in health and disease. *Nat. Rev. Neurosci.* 6, 449–462. doi: 10.1038/nrn1671
- Gozes, I., Helmsmoortel, C., Vandeweyer, G., Van der Aa, N., Kooy, F., and Sermone, S. B. (2015). The compassionate side of neuroscience: tony sermone's undiagnosed genetic journey—ADNP mutation. *J. Mol. Neurosci.* 56, 751–757. doi: 10.1007/s12031-015-0586-586
- Gozes, I., Sragovich, S., Schirer, Y., and Idan-Feldman, A. (2016). D-SAL and NAP: two peptides sharing a SIP domain. *J. Mol. Neurosci.* 59, 220–231. doi: 10.1007/s12031-015-0701-708
- Helmsmoortel, C., Vulto-van Silfhout, A. T., Coe, B. P., Vandeweyer, G., Rooms, L., van den Ende, J., et al. (2014). A SWI/SNF-related autism syndrome caused by de novo mutations in ADNP. *Nat. Genet.* 46, 380–384. doi: 10.1038/ng.2899
- Honnappa, S., Gouveia, S. M., Weisbrich, A., Damberger, F. F., Bhavesh, N. S., Jawhari, H., et al. (2009). An EB1-binding motif acts as a microtubule tip localization signal. *Cell* 138, 366–376. doi: 10.1016/j.cell.2009.04.065
- Honnappa, S., Okhrimenko, O., Jaussi, R., Jawhari, H., Jelesarov, I., Winkler, F. K., et al. (2006). Key interaction modes of dynamic +TIP networks. *Mol. Cell* 23, 663–671. doi: 10.1016/j.molcel.2006.07.013
- Huang, J., and Auchus, A. P. (2007). Diffusion tensor imaging of normal appearing white matter and its correlation with cognitive functioning in mild cognitive impairment and Alzheimer's disease. *Ann. N. Y. Acad. Sci.* 1097, 259–264. doi: 10.1196/annals.1379.021
- Huang, Y., Wu, Z., Cao, Y., Lang, M., Lu, B., and Zhou, B. (2014). Zinc binding directly regulates tau toxicity independent of tau hyperphosphorylation. *Cell Rep.* 8, 831–842. doi: 10.1016/j.celrep.2014.06.047
- Ivashko-Pachima, Y., and Gozes, I. (2018). NAP protects against tau hyperphosphorylation through GSK3. *Curr. Pharm. Des.* 24, 3868–3877. doi: 10.2174/1381612824666181112105954
- Ivashko-Pachima, Y., Maor-Nof, M., and Gozes, I. (2019). NAP (davunetide) preferential interaction with dynamic 3-repeat Tau explains differential protection in selected tauopathies. *PLoS One* 14:e0213666. doi: 10.1371/journal.pone.0213666
- Ivashko-Pachima, Y., Sayas, C. L., Malishkevich, A., and Gozes, I. (2017). ADNP/NAP dramatically increase microtubule end-binding protein-Tau interaction: a novel avenue for protection against tauopathy. *Mol. Psychiatry* 22, 1335–1344. doi: 10.1038/mp.2016.255
- Jiang, D., Sullivan, P. G., Sensi, S. L., Steward, O., and Weiss, J. H. (2001). Zn(2+) induces permeability transition pore opening and release of pro-apoptotic peptides from neuronal mitochondria. *J. Biol. Chem.* 276, 47524–47529. doi: 10.1074/jbc.M108834200
- Jiang, K., Toedt, G., Montenegro Gouveia, S., Davey, N. E., Hua, S., van der Vaart, B., et al. (2012). A Proteome-wide screen for mammalian SxIP motif-containing microtubule plus-end tracking proteins. *Curr. Biol.* 22, 1800–1807. doi: 10.1016/j.cub.2012.07.047
- Jouroukhin, Y., Ostritsky, R., Assaf, Y., Pelled, G., Giladi, E., and Gozes, I. (2013). NAP (davunetide) modifies disease progression in a mouse model of severe neurodegeneration: protection against impairments in axonal transport. *Neurobiol. Dis.* 56, 79–94. doi: 10.1016/j.nbd.2013.04.012
- Kanaan, N. M., Morfini, G., Pigino, G., LaPointe, N. E., Andreadis, A., Song, Y., et al. (2012). Phosphorylation in the amino terminus of tau prevents inhibition of anterograde axonal transport. *Neurobiol. Aging* 33, e815–e830. doi: 10.1016/j.neurobiolaging.2011.06.006
- Kanaan, N. M., Morfini, G. A., LaPointe, N. E., Pigino, G. F., Patterson, K. R., Song, Y., et al. (2011). Pathogenic forms of tau inhibit kinesin-dependent axonal transport through a mechanism involving activation of axonal phosphotransferases. *J. Neurosci.* 31, 9858–9868. doi: 10.1523/JNEUROSCI.0560-11.2011
- Kanaan, N. M., Pigino, G. F., Brady, S. T., Lazarov, O., Binder, L. I., and Morfini, G. A. (2013). Axonal degeneration in Alzheimer's disease: when signaling abnormalities meet the axonal transport system. *Exp. Neurol.* 246, 44–53. doi: 10.1016/j.expneurol.2012.06.003
- Kneynsberg, A., Combs, B., Christensen, K., Morfini, G., and Kanaan, N. M. (2017). Axonal degeneration in tauopathies: disease relevance and underlying mechanisms. *Front. Neurosci.* 11:572. doi: 10.3389/fnins.2017.00572
- Koh, J. Y., Suh, S. W., Gwag, B. J., He, Y. Y., Hsu, C. Y., and Choi, D. W. (1996). The role of zinc in selective neuronal death after transient global cerebral ischemia. *Science* 272, 1013–1016. doi: 10.1126/science.272.5264.1013
- Komarova, Y., De Groot, C. O., Grigoriev, I., Gouveia, S. M., Munteanu, E. L., Schober, J. M., et al. (2009). Mammalian end binding proteins control persistent microtubule growth. *J. Cell Biol.* 184, 691–706. doi: 10.1083/jcb.200807179
- Kowall, N. W., and Kosik, K. S. (1987). Axonal disruption and aberrant localization of tau protein characterize the neuropil pathology of Alzheimer's disease. *Ann. Neurol.* 22, 639–643. doi: 10.1002/ana.410220514
- Lee, M. C., Yu, W. C., Shih, Y. H., Chen, C. Y., Guo, Z. H., Huang, S. J., et al. (2018). Zinc ion rapidly induces toxic, off-pathway amyloid-beta oligomers distinct from amyloid-beta derived diffusible ligands in Alzheimer's disease. *Sci. Rep.* 8:4772. doi: 10.1038/s41598-018-23122-x
- Malishkevich, A., Marshall, G. A., Schultz, A. P., Sperling, R. A., Aharon-Peretz, J., and Gozes, I. (2016). Blood-borne activity-dependent neuroprotective protein (ADNP) is correlated with premorbid intelligence, clinical stage, and Alzheimer's disease biomarkers. *J. Alzheimers Dis.* 50, 249–260. doi: 10.3233/JAD-150799
- Merenlender-Wagner, A., Malishkevich, A., Shemer, Z., Udawela, M., Gibbons, A., Scarr, E., et al. (2015). Autophagy has a key role in the pathophysiology of schizophrenia. *Mol. Psychiatry* 20, 126–132. doi: 10.1038/mp.2013.174
- Minami, A., Sakurada, N., Fuke, S., Kikuchi, K., Nagano, T., Oku, N., et al. (2006). Inhibition of presynaptic activity by zinc released from mossy fiber terminals during tetanic stimulation. *J. Neurosci. Res.* 83, 167–176. doi: 10.1002/jnr.20714
- Moughamian, A. J., Osborn, G. E., Lazarus, J. E., Maday, S., and Holzbaur, E. L. (2013). Ordered recruitment of dynactin to the microtubule plus-end is required for efficient initiation of retrograde axonal transport. *J. Neurosci.* 33, 13190–13203. doi: 10.1523/JNEUROSCI.0935-13.2013
- Oz, S., Ivashko-Pachima, Y., and Gozes, I. (2012). The ADNP derived peptide, NAP modulates the tubulin pool: implication for neurotrophic and neuroprotective activities. *PLoS One* 7:e51458. doi: 10.1371/journal.pone.0051458
- Oz, S., Kapitansky, O., Ivashko-Pachima, Y., Malishkevich, A., Giladi, E., Skalka, N., et al. (2014). The NAP motif of activity-dependent neuroprotective protein (ADNP) regulates dendritic spines through microtubule end binding proteins. *Mol. Psychiatry* 19, 1115–1124. doi: 10.1038/mp.2014.97
- Rapsomaniki, M. A., Kotsantis, P., Symeonidou, I. E., Giakoumakis, N. N., Taraviras, S., and Lygerou, Z. (2012). easyFRAP: an interactive, easy-to-use tool for qualitative and quantitative analysis of FRAP data. *Bioinformatics* 28, 1800–1801. doi: 10.1093/bioinformatics/bts241
- Rasband, M. N. (2010). The axon initial segment and the maintenance of neuronal polarity. *Nat. Rev. Neurosci.* 11, 552–562. doi: 10.1038/nrn2852
- Sanchez-Martin, F. J., Valera, E., Casimiro, I., and Merino, J. M. (2010). Nerve growth factor increases the sensitivity to zinc toxicity and induces cell cycle arrest in PC12 cells. *Brain Res. Bull.* 81, 458–466. doi: 10.1016/j.brainresbull.2009.11.008
- Sayas, C. L., Tortosa, E., Bollati, F., Ramirez-Rios, S., Arnal, I., and Avila, J. (2015). Tau regulates the localization and function of End-binding proteins 1 and 3 in developing neuronal cells. *J. Neurochem.* 133, 653–667. doi: 10.1111/jnc.13091
- Schindelin, J., Arganda-Carreras, I., Frise, E., Kaynig, V., Longair, M., Pietzsch, T., et al. (2012). Fiji: an open-source platform for biological-image analysis. *Nat. Methods* 9, 676–682. doi: 10.1038/nmeth.2019
- Schrödinger, L. (2015). *The PyMOL Molecular Graphics System, Version 2.0.*
- Sensi, S. L., Paoletti, P., Bush, A. I., and Sekler, I. (2009). Zinc in the physiology and pathology of the CNS. *Nat. Rev. Neurosci.* 10, 780–791. doi: 10.1038/nrn2734

- Sensi, S. L., Paoletti, P., Koh, J. Y., Aizenman, E., Bush, A. I., and Hershfinkel, M. (2011). The neurophysiology and pathology of brain zinc. *J. Neurosci.* 31, 16076–16085. doi: 10.1523/JNEUROSCI.3454-11.2011
- Shiryaev, N., Pikman, R., Giladi, E., and Gozes, I. (2011). Protection against tauopathy by the drug candidates NAP (davunetide) and D-SAL: biochemical, cellular and behavioral aspects. *Curr. Pharm. Des.* 17, 2603–2612. doi: 10.2174/138161211797416093
- Shuttleworth, C. W., and Weiss, J. H. (2011). Zinc: new clues to diverse roles in brain ischemia. *Trends Pharmacol. Sci.* 32, 480–486. doi: 10.1016/j.tips.2011.04.001
- Vulih-Shultzman, I., Pinhasov, A., Mandel, S., Grigoriadis, N., Touloumi, O., Pittel, Z., et al. (2007). Activity-dependent neuroprotective protein snippet NAP reduces tau hyperphosphorylation and enhances learning in a novel transgenic mouse model. *J. Pharmacol. Exp. Ther.* 323, 438–449. doi: 10.1124/jpet.107.129551
- Yang, M. H., Yang, Y. H., Lu, C. Y., Jong, S. B., Chen, L. J., Lin, Y. F., et al. (2012). Activity-dependent neuroprotector homeobox protein: a candidate protein identified in serum as diagnostic biomarker for Alzheimer's disease. *J. Proteomics* 75, 3617–3629. doi: 10.1016/j.jprot.2012.04.017
- Zamostiano, R., Pinhasov, A., Bassan, M., Perl, O., Steingart, R. A., Atlas, R., et al. (1999). A femtomolar-acting neuroprotective peptide induces increased levels of heat shock protein 60 in rat cortical neurons: a potential neuroprotective mechanism. *Neurosci. Lett.* 264, 9–12. doi: 10.1016/s0304-3940(99)00168-8

Conflict of Interest: IG serves as the Chief Scientific Officer of Coronis Neurosciences, developing CP102 (SKIP and Ac-SKIP) for neurological disorders.

The remaining author declares that the research was conducted in the absence of any commercial or financial relationships that could be construed as a potential conflict of interest.

Copyright © 2019 Ivashko-Pachima and Gozes. This is an open-access article distributed under the terms of the Creative Commons Attribution License (CC BY). The use, distribution or reproduction in other forums is permitted, provided the original author(s) and the copyright owner(s) are credited and that the original publication in this journal is cited, in accordance with accepted academic practice. No use, distribution or reproduction is permitted which does not comply with these terms.